J. Fluid Mech. (1974), *vol.* 66, *part* 1, *pp.* 107–113
Printed in Great Britain

Axisymmetric expansion of a gas from a nozzle into a vacuum

By THOMAS W. TUER† AND GEORGE S. SPRINGER

Fluid Dynamics Laboratory, Department of Mechanical Engineering, University of Michigan, Ann Arbor

(Received 3 December 1973)

Using a test-particle Monte Carlo method the general features of a gas expanding from a circular nozzle into a vacuum were investigated. Calculations were performed by considering the flow to be uniform and axial at the exit plane of the nozzle with an exit Mach number of 3 and a throat Reynolds number of 25. Results are presented for the density, mean flow velocity and kinetic temperature of the gas. Near the axis of the jet the calculated density distributions were found to agree well with those given by Robertson & Willis. Results are also presented for regions far from the jet's axis where no other solution is available.

1. Introduction

Although the problem of the expansion of a gas from a nozzle into a vacuum is of considerable basic and practical interest, relatively few results describing such flows are available. Robertson & Willis (1971) and Peracchio (1970) obtained solutions applicable near the axis of the jet ($\theta < 40°$, figure 1), while Grier (1969) presented an approximate solution which applies only at large distances from the axis ($\theta > 90°$). No results seem to be available between these two regions. The objective of this investigation was to study the general features of a gas issuing from a nozzle into a vacuum with emphasis on the region of the flow where results did not exist ($40° < \theta < 90°$). The results presented here were generated by a Monte Carlo procedure. The particular problem considered is described in the next section.

2. Statement of the problem

A gas, assumed to be ideal and obeying Maxwell's inverse-fifth-power law of repulsion, discharges into a vacuum from a circular nozzle of radius r_e (figure 1). The gas density n_e, mean flow velocity u_e and the temperature T_e over the exit plane of the nozzle are taken to be uniform (i.e. boundary-layer effects are neglected). At the exit plane, the mean flow velocity is considered to be axial (i.e. $u_{ze} = u_e$, $u_{re} = u_{\theta e} = 0$). For this problem the following quantities were determined: the molecular number density n/n_0, the axial and radial components u_z/c_0 and u_r/c_0 of the mean flow velocity, and the axial, radial and azimuthal

† Present address: Science Applications, Inc., P.O. Box 328, Ann Arbor, Michigan 48107.

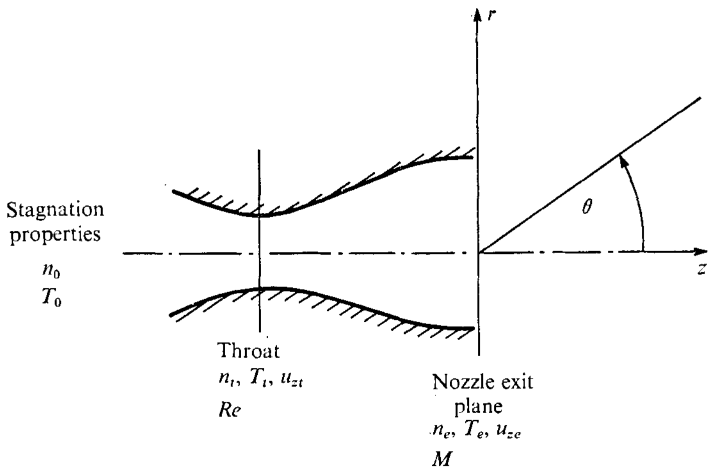

FIGURE 1. The co-ordinate system used in the analysis.

components T_z/T_0, T_r/T_0 and T_ϕ/T_0 of the kinetic temperature. The ith component of the kinetic temperature is defined as $nRT_i = \langle v_i^2\rangle - \langle v_i\rangle^2$, where v_i is the molecular velocity and R is the gas constant. c_0 is the thermal velocity $[c_0 = (2RT_0)^{\frac{1}{2}}]$. The subscript zero denotes stagnation conditions. The foregoing quantities were evaluated as functions of the axial and radial distances $z^* = z/r_e$ and $r^* = r/r_e$ from the centre of the exit plane of the nozzle.

Although n_e, u_{ze} and T_e are required as boundary conditions for the Monte Carlo solution, the problem is usually specified in terms of the Mach number M at the exit plane and the Reynolds number Re at the throat of the nozzle:

$$M \equiv u_{ze}/(\gamma RT_e)^{\frac{1}{2}}, \quad Re \equiv mn_t(2r_t)\,u_{zt}/\mu_t. \tag{1}$$

The subscript t refers to conditions at the throat. γ is the ratio of specific heats, m is the molecular weight and μ is the dynamic viscosity:

$$\mu_t = \{mRT_t/[3\pi A_2(4)]\}\,(2m/\kappa)^{\frac{1}{2}}, \tag{2}$$

where $A_2(4)$ and κ are molecular constants. If the flow is assumed to be one-dimensional and isentropic inside the nozzle, n_e, u_{ze} and T_e can be directly related to M and Re. Using the isentropic relations given by Shapiro (1953), the temperature and velocity at the exit plane may be expressed (for $\gamma = \frac{5}{3}$) as

$$T_e^* \equiv T_e/T_0 = (1+\tfrac{1}{3}M^2)^{-1}, \tag{3}$$

$$u_{ze}^* \equiv u_{ze}/(2RT_0)^{\frac{1}{2}} = M[5/(6+2M^2)]^{\frac{1}{2}}. \tag{4}$$

The density at the exit plane can be related to the density n_t at the throat by the isentropic relation

$$n_e = 8n_t/(3+M^2)^{\frac{3}{2}}. \tag{5}$$

n_t may be obtained from (1) and (2):

$$n_t = \{RT_t/[6\pi A_2(4)]\}\,(2m/\kappa)^{\frac{1}{2}}\,Re/(r_t u_{zt}). \tag{6}$$

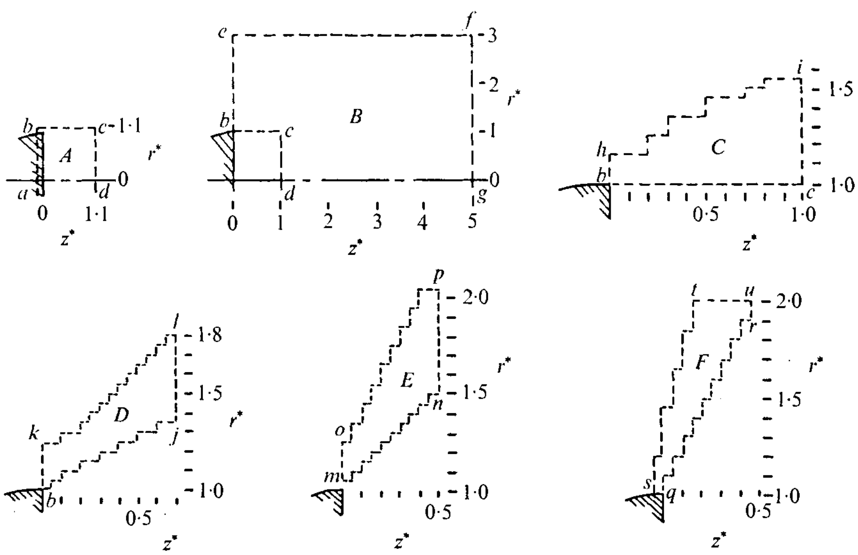

FIGURE 2. Control volumes used in the calculations.

The parameters r_t, T_t and u_{zt} at the throat (where $M = 1$) are also obtained by assuming isentropic flow, i.e.

$$r_t/r_e = (A_t/A_e)^{\frac{1}{2}} = 4M^{\frac{1}{2}}/(3+M^2), \tag{7}$$

$$T_t/T_0 = \tfrac{3}{4}, \quad u_{zt}/(2RT_0)^{\frac{1}{2}} = (\tfrac{5}{8})^{\frac{1}{2}}. \tag{8), (9}$$

Equations (5)–(9) may be combined to yield

$$n_e^* \equiv n_e r_e^3 = [Re/2\pi A_2(4)]\,[\kappa^*(5M)\,(3+M^2)]^{-\frac{1}{2}}. \tag{10}$$

Equations (3), (4) and (10) provide the necessary relationships between n_e, T_e and u_{ze} (or their dimensionless forms n_e^*, T_e^* and u_{ze}^*) and Re and M. The numerical value of $A_2(4)$ is 0·436. The parameter $\kappa^* \equiv (\kappa/m)\,(2RT_0 r_e^4)^{-1}$ was taken to be 0·01402 (Tuer & Springer 1974).

3. Control volumes

A control volume is defined here as that portion of the flow field which is being considered in any particular Monte Carlo calculation. In the present study six different control volumes were used (figure 2), because of the large density gradients present in the flow field of interest. These control volumes overlapped, so that the boundary conditions for adjacent control volumes could be matched. Control volumes A and B were used to determine the characteristics of the flow field near the axis; control volumes C–F were used to obtain details of the flow at large angles from the axis.

Control volume A was divided into 132 cells in the shape of cylindrical annuli. Each cell had a length $\Delta z^* = 0{\cdot}1$ and thickness $\Delta r^* = 0{\cdot}1$. A portion of the control volume consisting of a single row of ten cells was placed inside the nozzle (i.e.

the region $-0{\cdot}1 \leqslant z^* \leqslant 0$, $0 \leqslant r^* \leqslant 1$). These ten cells were used as 'reference cells' in the Monte Carlo density calculation. The densities of the gas in each of the reference cells were taken to be equal to the value n_e at the exit plane. Furthermore, the flow parameters of the gas were taken to be uniform throughout the ten reference cells, and the velocity and temperature at the upstream boundary of the reference cells ($z^* = -0{\cdot}1$, $0 \leqslant r^* \leqslant 1$) were taken to be the values u_{ze} and T_e at the exit plane.

By placing the reference cells inside the nozzle, a portion of the inside surface of the nozzle ($r^* = 1$, $-0{\cdot}1 \leqslant z^* \leqslant 0$) became a boundary of the control volume. For the Monte Carlo procedure the accommodation coefficient F at this surface must be specified. For convenience, specular reflexion ($F = 0$) was assumed.

The upstream faces of the reference cells ($z^* = -0{\cdot}1$, $0 \leqslant r^* \leqslant 1$) were employed as 'entrance faces' to the control volume. The fluxes of molecules through each of these ten entrance faces were equal. Thus, the number N_i of test particles introduced into the control volume via each entrance face was proportional to the area of that face. In the calculations the following values were used: $N_i = 18$, 54, 90, 126, 162, 198, 234, 270, 306, 342, for $i = 1, 2, 3, \ldots, 10$, counted radially outwards from the central entrance face.

The flow at the 'outer boundaries' of this control volume (i.e. the surface generated by revolving *bcd* in figure 2) was taken to be hypersonic (no incoming flow).

Control volumes *B*–*F* were divided into cells in the form of coaxial annuli. The length and thickness of the cells were $\Delta z^* = 0{\cdot}5$ and $\Delta r^* = 0{\cdot}5$ in control volume *B* and $\Delta z^* = 0{\cdot}05$ and $\Delta r^* = 0{\cdot}05$ in control volumes *C*–*F*.

The 'inner boundary conditions' for control volumes *B* and *C* (i.e. along *bcd* and along *bc* in figure 2) were determined from the results for control volume *A*. Similarly, the results for *C* were used as inner boundary conditions for *D* (along *bj*), the results for *D* as inner boundary conditions for *E* (along *mn*) and the results for *E* as inner boundary conditions for *F* (along *qr*). The 'outer boundary conditions' for control volumes *B*–*F* (along surfaces *befg*, *bhic*, *bklj*, *mopn* and *stur*) were based on the hypersonic approximation.

For the first run for each of these control volumes, all intermolecular collisions were suppressed by artificially specifying a very small density as an initial estimate in each cell. By this procedure, no other initial estimates were necessary.

4. Results

The results were obtained using a test-particle Monte Carlo procedure. The details of this procedure have been described previously (Tuer & Springer 1974) and therefore are not repeated here. Results were obtained for an exit Mach number $M = 3$ and throat Reynolds number $Re = 25$. These values are the same as those used by Robertson & Willis (1971) in their analytical solution of this problem. Thus, the use of these values enables us to compare some of our results with those of Robertson & Willis.

The calculated density, velocity and temperature distributions are shown in figures 3–6. In figure 3 the density distributions calculated by Robertson &

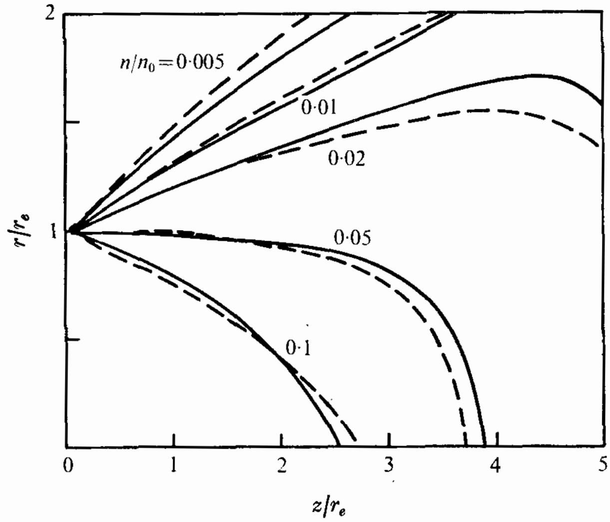

FIGURE 3. Number density as a function of distance from nozzle exit. ——, present results; – – –, Robertson & Willis (1971). (M = 3, Re = 25.)

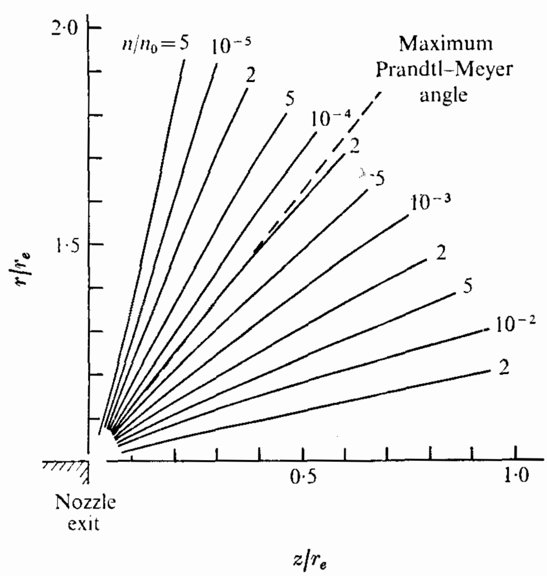

FIGURE 4. Number density as a function of distance from nozzle exit. (M = 3, Re = 25.)

Willis are also included. Note that these investigators considered only a region extending from the axis to about 40° from the axis, and from the nozzle out to about ten nozzle radii. The present density calculations agree well with those of Robertson & Willis. Some of the minor differences in the two sets of results may be attributed to the difficulty in taking readings from the small graphs presented by Robertson & Willis. The radial, axial and azimuthal temperature distributions shown in figure 6 are also similar in shape to those given by Robertson &

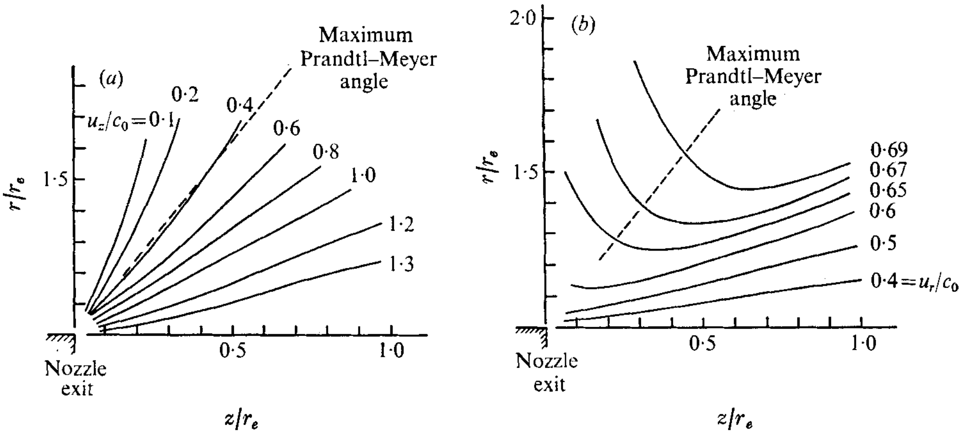

FIGURE 5. (*a*) Axial and (*b*) radial components of the mean flow velocity as functions of distance from nozzle exit. ($M = 3$, $R = 25$.)

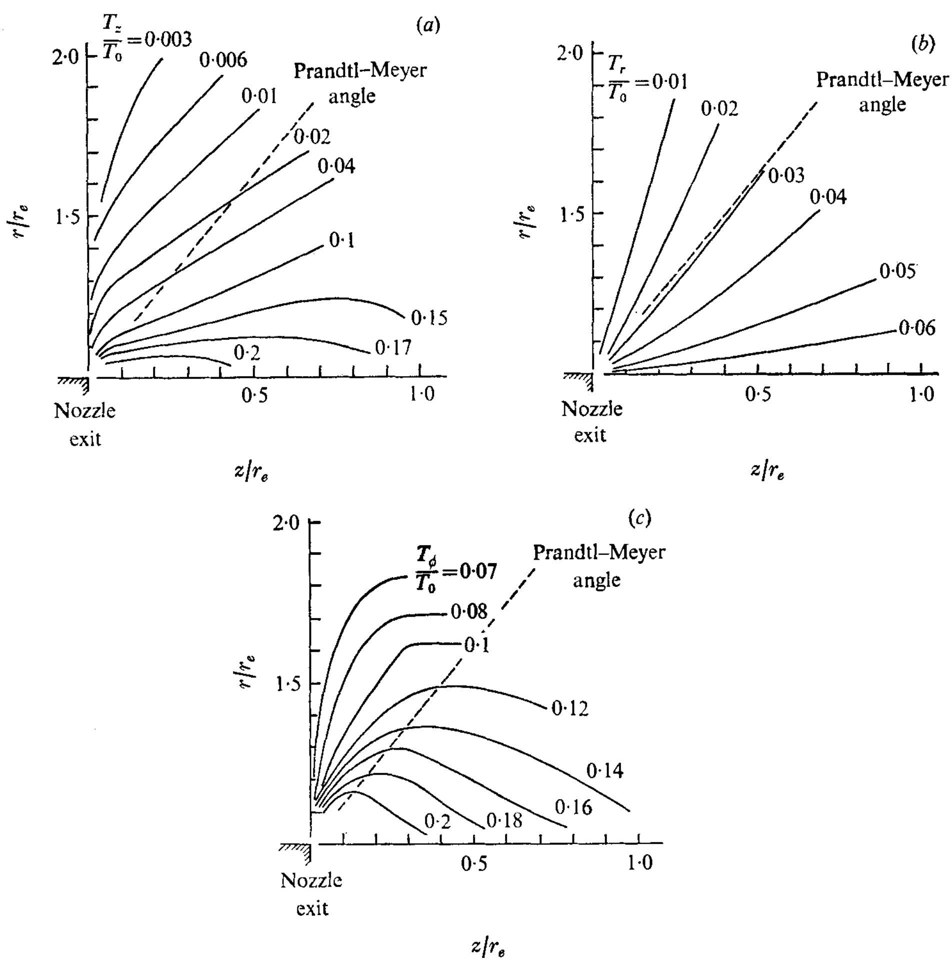

FIGURE 6. (*a*) Axial, (*b*) radial and (*c*) azimuthal components of kinetic temperature as functions of distance from nozzle exit. ($M = 3$, $Re = 25$.)

Willis. Unfortunately, the scales on their graphs are such that a qualitative comparison with the present results is not possible. Velocities were not calculated by Robertson & Willis.

The flow expanding from a circular nozzle into a vacuum was also investigated by Grier (1969). Grier studied only the region ahead of the plane of the nozzle (i.e. $z < 0$, $r/r_e \geqslant 1$; see figure 1). Thus, the present results (where $z > 0$) cannot be compared directly with those of Grier.

It is noteworthy that the density distributions calculated by the present Monte Carlo technique indicate gas to be present in the region beyond the limiting Prandtl–Meyer angle of continuum theory (figure 4). This is in qualitative agreement with the analytical results of Peracchio (1970) (for a two-dimensional nozzle) and Grier (1969), which show that gas is scattered into the region where continuum theory predicts a void.

The mean flow velocity in the axial direction decreases with the angle from the axis (figure 5*a*). Physically, this component of velocity must tend to zero as 90° is approached, and eventually become negative. The mean flow velocity in the radial direction is relatively uniform (figure 5*b*).

The axial component of the kinetic temperature displays a rapid decay with the angle θ from the axis (figure 6*a*). At small θ, the radial component of temperature has a much lower value than the axial component (figure 6*b*). However, the magnitude of the radial component decays more slowly than that of the axial component. At large angles from the axis the radial component actually becomes larger than the axial one. The azimuthal component of kinetic temperature has a completely different profile from the other two components and is larger than the other two at all angles (figure 6*c*). This is different from the behaviour of flows expanding from spherical point or cylindrical line sources, where at a given point the radial component of the temperature is always larger than the other two components (Bird 1970).

Although the foregoing results are only for one representative Mach number and one representative Reynolds number, the results do indicate the general features of the flow field, including the density, velocity and temperature distributions. It would be desirable to extend the calculations to other conditions but, owing to the expense involved (approximately 90 min on the IBM 360/67 computer), additional computations have not yet been performed.

This work was supported by the McDonnell-Douglas Astronautics Company.

REFERENCES

Bird, G. A. 1970 *A.I.A.A. J.* **8**, 1998.

Grier, N. T. 1969 In *Rarefied Gas Dynamics* (ed. Trilling & Wachman), p. 895. Academic.

Peracchio, A. A. 1970 *A.I.A.A. J.* **8**, 1965.

Robertson, S. J. & Willis, D. R. 1971 *A.I.A.A. J.* **9**, 291.

Shapiro, A. H. 1953 *Compressible Fluid Flow*, vol. 1, chap. 4. Ronald Press Co.

Tuer, T. W. & Springer, G. S. 1974 *Computers & Fluids*, **1**, 399.